Δελτίο της Ελληνικής Γεωλογικής Εταιρίας, τόμος L, σελ. 383-391
Πρακτικά 14ου Διεθνούς Συνεδρίου, Θεσσαλονίκη, Μάιος 2016

Bulletin of the Geological Society of Greece, vol. L, p. 383-391
Proceedings of the 14th International Congress, Thessaloniki, May 2016

RECENT SEDIMENTARY PROCESSES IN THE WESTERN GULF OF CORINTH, GREECE: SEISMIC AND ASEISMIC TURBITIDES

Sergiou S.[1], Beckers A.[2], Geraga M.[1], Papatheodorou G.[1], Iliopoulos I.[3] and Papaefthymiou H.[4]

[1]University of Patras, Department of Geology, Laboratory of Marine Geology and Physical Oceanography 26 504, Patras, Greece, sergiou@upatras.gr, mgeraga@upatras.gr, gpapathe@upatras.gr

[2]Department of Geography, University of Liège, Liège B-4000, Belgium, abeckers@ulg.ac.be

[3]University of Patras, Department of Geology 26 504, Patras, Greece, morel@upatras.gr

[4]University of Patras, Department of Chemistry 26 504, Patras, Greece, epap@chemistry.upatras.gr

Abstract

The Corinth rift is counted among the most active tectonic grabens in the world, with extension rates up to 15 mm/yr (Western part). These high extension rates are associated with very strong seismic events that are, occasionally, responsible for submarine mass movements. These movements, their consequential bottom currents, and the differential river-discharging sediment accumulation in the whole gulf, strongly affect the modern marine sedimentary processes. The definition and understanding of these processes is the main aim of this project. This is attempted through via sedimentological, mineral and geochemical analyses on sediment samples from two ~1.1 m long, sediment cores from a WE submarine canyon (10 km long, 3 km wide) that lies in the Western tip of the gulf. The general sedimentation motif reveals the presence of hemipelagic deposits which are occasionally interrupted by sandy turbidites. Occasionally, these turbidites seem to have seismic origin. The sedimentation rates range between 2.57 mm/yr in the western part and 0.67 mm/yr in the eastern part.

Keywords: *marine sediments, submarine mass movements, seismic and aseismic turbidites, age model.*

Περίληψη

Η παρούσα εργασία στοχεύει στην μελέτη και ανάδειξη των σύγχρονων διεργασιών ιζηματογένεσης στον δυτικό Κορινθιακό κόλπο μέσα από μια σειρά εργαστηριακών αναλύσεων σε ιζήματα πυρήνων ιζήματος. Δύο πυρήνες βαρύτητας μήκους περίπου 1 μ. από την περιοχή ενός υποθαλάσσιου καναλιού μεταφοράς ιζημάτων επιλέχθηκαν προς ανάλυση. Σε αυτούς μελετήθηκαν οι ιζηματογενείς ιστολογικές δομές μέσω οπτικών παρατηρήσεων και ακτινογραφήσεων (X rays), η κοκκομετρική κατανομή και η ορυκτολογική σύσταση των ιζημάτων τους, ενώ πραγματοποιήθηκαν επίσης χημικές αναλύσεις προσδιορισμού της φυσικής ραδιενέργειας (^{226}Ra, ^{232}Th, ^{40}K) και ραδιοχρονολογήσεις (^{14}C). Η σύνθεση όλων των παραπάνω, φανερώνει το μοντέλο

ιζηματογένεσης του καναλιού κατά το οποίο, ημιπελαγικές ακολουθίες διακόπτονται από αμμώδεις τουρβιδίτες οι οποίοι ενίοτε αποτελούν συνέπεια κάποιου σεισμικού γεγονότος (σεισμικοί τουρβιδίτες). Τα θαλάσσια ρεύματα της περιοχής, ο τεκτονισμός, και οι παροχές των ποταμών που εκβάλουν στον δυτικό Κορινθιακό κόλπο, επηρεάζουν καθοριστικά τις διεργασίες και τον ρυθμό ιζηματογένεσης ο οποίος μειώνεται προς τα ανατολικά κατά μήκος του καναλιού από 2.57 mm/yr σε 0.67 mm/yr.
Λέξεις κλειδιά: *θαλάσσια ιζήματα, υποθαλάσσιες βαρυτικές μετακινήσεις, τουρβιδίτες, σεισμική στρωματογραφία.*

1. Introduction

The Corinth rift represents one of the most active intra-continental rifts on earth, with high levels of seismicity and rapid extension (Papazachos and Comninakis, 1971; McKenzie, 1972, 1978; Makris, 1976; Doutsos *et al*., 1988; Jackson and McKenzie, 1988).This rift which is 115 km long and NE-trending separates the central Greece to the north from the Peloponnese to the south (Fig. 1). Fan delta prograding deposits during Pleistocene sea-level changes, are the predominant sedimentary processes in the steep flanks of the gulf (Ferentinos *et al*., 1988; Perissoratis *et al*., 2000; Lykousis *et al.*, 2007b). These processes are mostly related to seismically triggered gravitative mass movements (Piper *et al*., 1990; Ferentinos *et al*., 1988; Papatheodorou and Ferentinos, 1997).

The highest extensional rate (up to 15 mm yr^{-1}) has been recorded at the western tip of the Corinth Rift, where the geodetic measurements show that most of the present-day deformation is concentrated in a narrow band offshore (Briole *et al*., 2000; Avallone *et al*., 2004).

This high extensional regime is associated with intense seismic events that leave their imprints in the texture of the sediments which cover the sea-floor of that area (Ferentinos *et al.*, 1988; Heezen *et al*., 1966; Lykousis *et al.*, 2007b; Poulos *et al*., 1996). As a result, the earthquake history of the area could be revealed by investigating the sedimentary processes and deposits. Despite that, the study of the recent sediments in the western gulf of Corinth is important in the better understanding of the evolution of the sedimentation regime over the last 1000 years providing information regarding the mineralogy, the concentration of natural radionuclides and the distribution of the fluvial discharges from rivers with high terrigenous sediment supply, such as Mornos and Erineos rivers.

This work focuses on a WE-trending submarine canyon (10 km long, 3 km wide) that lies in the western tip of the gulf and acts as an active path of sediment transportation initially to the ‘’Delphic Plateau’’(Heezen *et al*., 1966) and, then finally, to the central basin (Fig. 1). This canyon has been formed by the tectonic subsistence of the north-dipping Psathopyrgos-Lambiri-Helike faults and the south-dipping Trizonia fault (Zelilidis, 2003) and is associated with gravitative mass movements during the late Quaternary (Heezen *et al*., 1966). For this canyon, Beckers (2015) has proposed different sedimentation rates ranging between 2.1-2.6 mm/yr in the western part and 0.8-1.6 mm/yr in the eastern part, based on radiocarbon dates from four sediment cores and two unsupported ^{210}Pb activity profiles.

2. Materials and Methods

For the present work, a series of sedimentological, mineralogical and geochemical analyses was performed on the sediments of two cores (CAN01UP, CAN03UP) retrieved by a BENTHOS gravity corer on the western and eastern part of the canyon, respectively (Fig. 1). The coring survey carried out within the framework of the “Siscor project: Seismicity in the western gulf of Corinth” (collaboration with the *ISTerre - Insitute of Earth Sciences-, Universite de Savoie and the Department of Geography, University of Liège)*.

The macroscopic description of the cores on the basis of color and texture together with the X-rays radiographs performed on core segments provided information of the sedimentary structures and the identification of the coarse and fine grained layers. Grain-size analyses were conducted with a laser

diffraction microgranulometer MALVERN™ Mastersizer 2000. The sampling interval for these analyses was 1cm throughout the cores and 0.5cm within selected sandy turbidites (event deposits). Mean size (Mz) and Standard deviation (σi) were also calculated.

In addition, in the sediments from the lithological units determined by the preceding analyses, X-ray diffraction was performed in order to determine the mineralogy and the activities of ^{226}Ra, ^{232}Th, and ^{40}K (NORM) were obtained by direct γ-ray spectroscopy.

Finally, radiocarbon (^{14}C) datings were performed in two sediment samples, one from each core, aiming to the estimation of: (i) the sedimentation rates in the canyon and (ii) the age of the turbidite deposits.

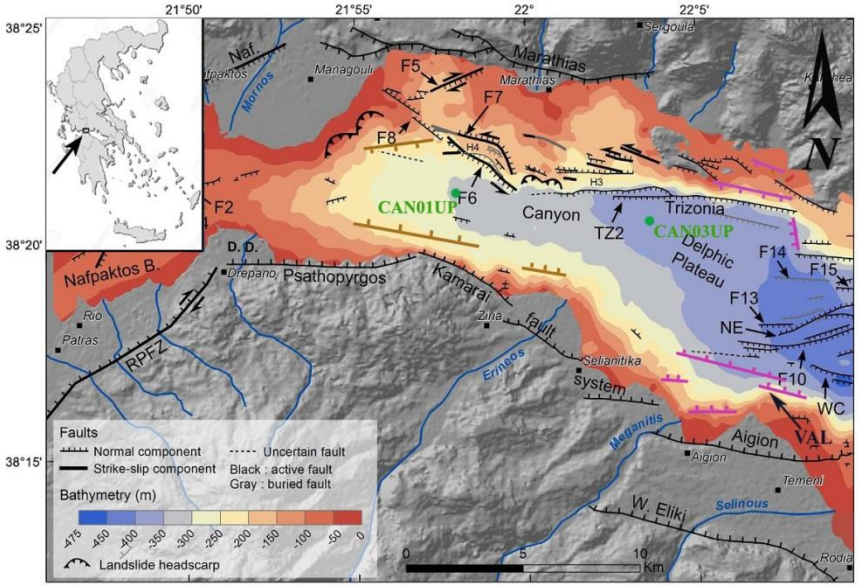

Figure 1 - Bathymetric-tectonic map of the investigated area. The coring sites are presented with green color. The river network is also depicted (after Beckers *et al.*, 2015; Moretti *et al.*, 2003; Stefatos *et al.*, 2002).

3. Results

3.1 Sedimentary motif and turbidites identification

The sedimentary motif for both cores reveals a sequence of hemipelagic deposits; silty and muddy sediments with high concentration of phyllosilicates, occasionally interrupted by sandy turbiditic layers (Fig. 2, 3). The turbiditic layers were identified by means of their physical properties such as the grain-size distribution and color, as these proxies show characteristic differences in the turbidites and the hemipelagic sediments. A ‘’sandy turbidite’’ refers to a coarse grain-size (coarse silt to sand) and poorly sorted massive layer that results from a turbidity current and represents a sediment layer that differs greatly from the silty hemipelagic background sedimentation. In the present study, the turbidites show clear normal grading and sharp boundaries to the over- and underlying sediments, which facilitates their difference from the hemipelagic facies. All the turbiditic layers show a distinct sharp, in most cases planar, basal contact. Some of the contacts have erosional surfaces and/or they were slightly deformed. In some cases, the upper limit of the turbidites layers is poorly defined, introducing difficulties to the determination of the boundary between turbiditic and hemipelagic sedimentation. The different sediment fractions can be also distinguished based on their color: the sandy turbidites deposits are often dark grayish due to the presence of organic material (mainly plant

residues) while the silty hemipelagic facies are lighter grayish brown. Quartz and feldspars are the dominant minerals within the turbidites deposits. Calcite and phyllosilicates are also present. A remarkable decrease of the concentration of natural radionuclides has been observed in the turbidites deposits compared to the hemipelgic deposits.

The layer thickness between the individual turbidites varies considerably and ranges from 0.5 to 7cm. Several thin turbidites show multiple sedimentation pulses preventing the counting of the individual turbidites layers. Moreover, radiographs reveal that the thicker turbidites are faintly laminated.

Based on the above presented characteristics all the sedimentary layers corresponding to turbidite deposits were determined. Fifteen (15) turbidites deposits (E1-E15) were identified within the CAN01UP and eleven (11) deposits (E1-E11) within the CAN03UP (Fig. 4). The sum thickness of all these layers reach up to 13 cm and 17 cm, in CAN01UP and CAN03UP cores, respectively, suggesting that the undisturbed hemipelagic sediments counts for the 88% and 84% of the total sedimentary material of CAN01UP and CAN03UP cores, respectively.

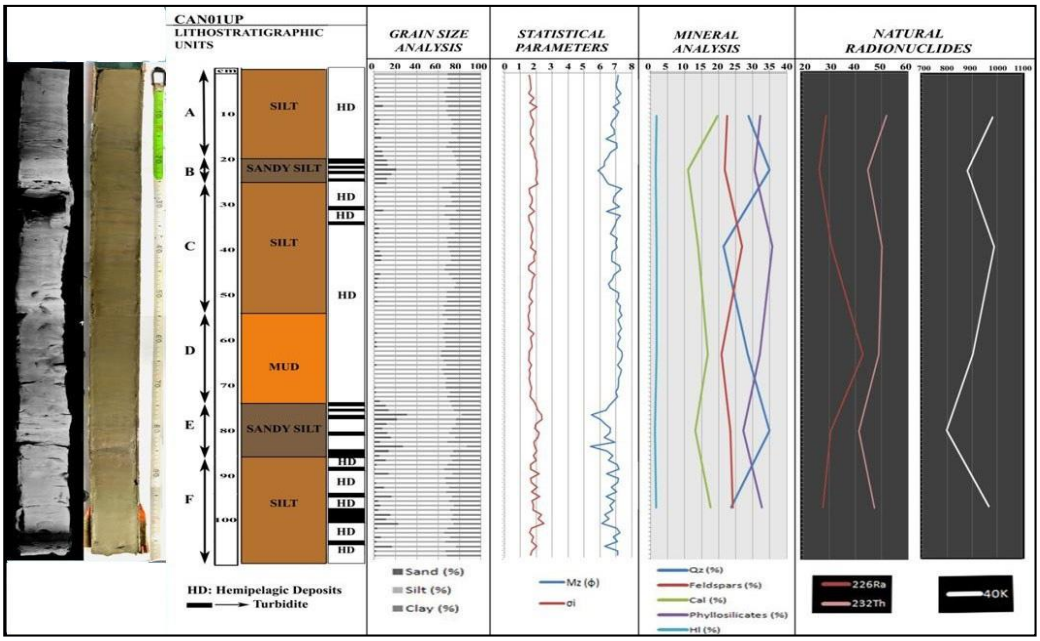

Figure 2 - Digital X-ray, RGB image and lithostratigraphy of CAN01UP accompanied by the downcore variations in the grain-size properties and the results of the mineralogical and geochemical (NORM) analyses.

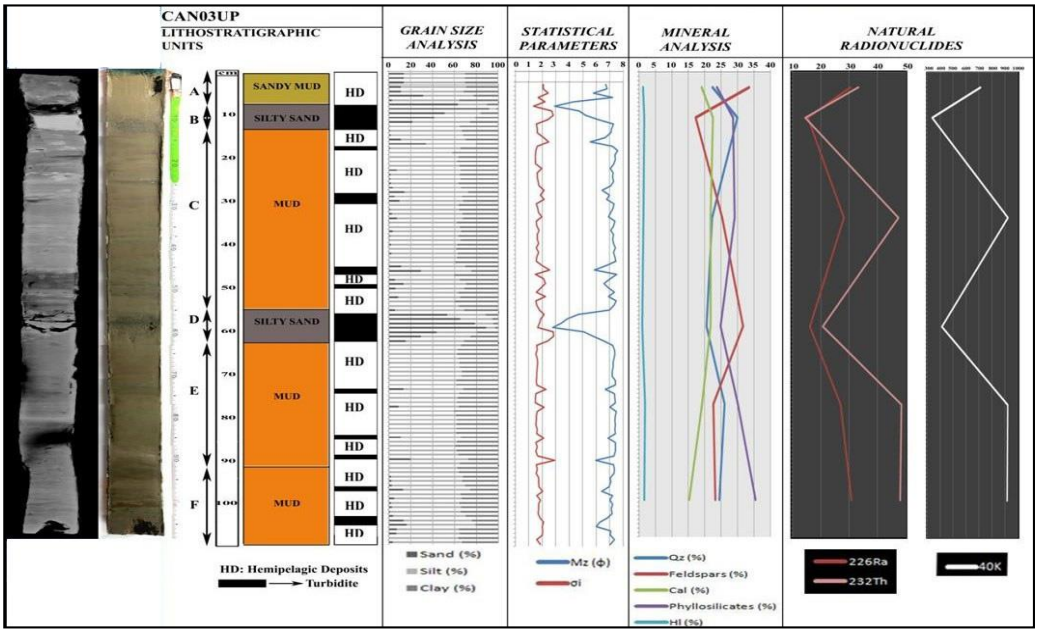

Figure 3 - Digital X-ray, RGB image and lithostratigraphy of CAN03UP accompanied by the downcore variations in the grain-size properties and the results of the mineralogical and geochemical (NORM) analyses.

3.2 Age models, sedimentation rates and seismic turbidites

The samples for the datings were carefully chosen from layers of hemipelagic sediments, obtained at 98.5 cm in the CAN01UP and at 89 cm in the CAN03UP core. These samples provided an age of 270±30 cal yrs BP for the CAN01UP core and an age of 953±28 cal yrs BP for the CAN03UP (Fig. 4).

The chronological framework of each core was suggested through the estimation of the depositional rate of the hemipelagic sedimentation. This rate was estimated by the extraction of all the turbiditic deposits occurred along each core and the application of linear extrapolation of the obtained age, assuming a steady hemipelagic sedimentation rate, at the remnant hemipelagic facies. The suggested age models showed that the CAN01UP core represents a time period of 382 yrs (1632 AD -2014) and the CAN03UP core a longer period of 1201 yrs (813 AD- 2014).

Furthermore these age models allowed us to estimate two different sedimentation rates; 2.57 mm/yr at the western part (CAN01UP) and 0.67 mm/yr at the eastern part (CAN03UP) of the canyon (Fig.4).

In CAN01UP sediment core, the age model showed that there are two main periods of evolution of the turbidity activity: (i) between 1869-1937 AD, having a frequency of 1 turbidity event/11yrs and (ii) between 1632-1742 AD with a frequency of 1 turbidity event /12yrs. In CAN03UP, due to the lower hemipelagic sedimentation rate, the periods of turbidity activity were less pronounced but they could imply three main periods: (iii) between 813-1240 AD the turbidity activity frequency is 1t.e/ 85yrs, (iv) between 1347-1507AD the frequency is 1t.e/53yrs and (v) between 1674-1923 AD the frequency is 1t.e/83yrs.

If we compare the suggested age of the turbidity events obtained from the two cores with the records of the earthquake history of the area (http://www.emidius.eu/SHEEC/, Papadopoulos, 2003) then ten (10) out of twenty six (26) turbidity events presents synchronicity with strong earthquakes of magnitude higher than 5.8. More specific, it seems that six (6) turbidites within the sedimentary record of the CAN01UP core were triggered by the 1660, 1703, 1714, 1742, 1889 and 1909 AD

earthquakes and four (4) within CAN03UP were triggered by the 1462, 1703, 1831 and 1909 AD earthquakes (Fig. 4).

The comparison of the seismic turbidite events (E) between the two cores showed that only two cases present similarities on the basis of their age and laboratory analyses (grain size measurements, sedimentary structures and the mineralogical and geochemical signature). E5 in CAN01UP and E1 in CAN03UP most probably were triggered by the same earthquake happened at 1888, 1909 or 1917 AD and E12 in CAN01UP and E3 in CAN03UP of one of the earthquakes of 1703 or 1714 AD (Fig. 4).

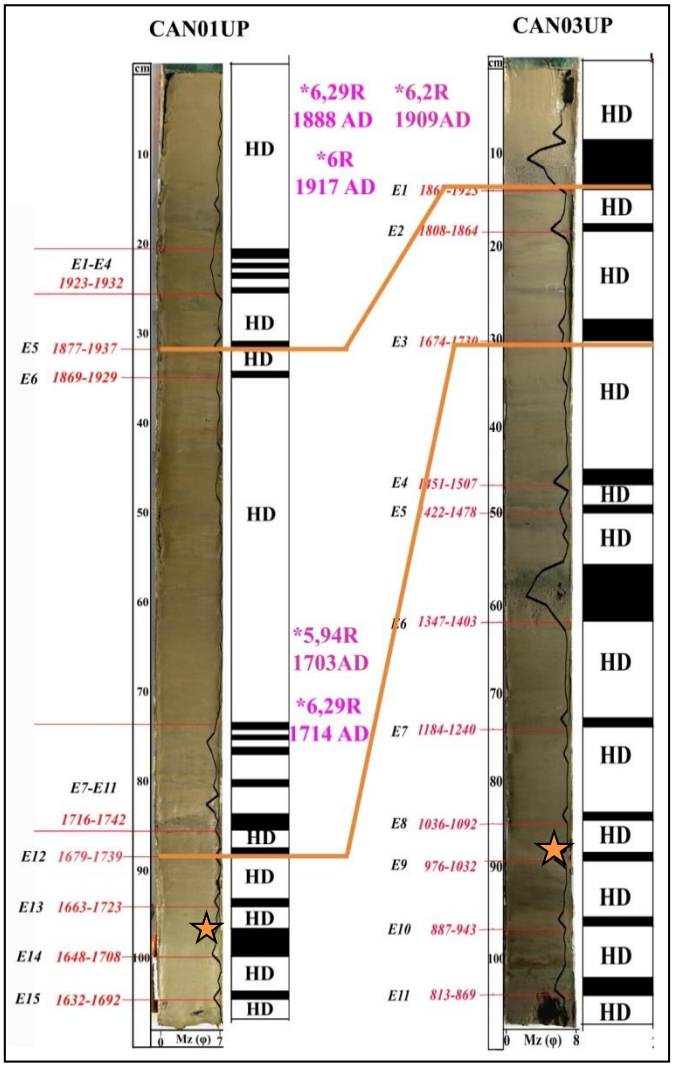

Figure 4 - Age model, turbidite events (E), hemipelagic sediments (HD) and the two stratigrafically correlated turbidite horizons. The sampling of the radiocarbon dating is indicated by stars.

Table 1 - Grain size characteristics, mineralogical and geochemical data of the two stratigraphically correlated seismic turbidite horizons.

Events		Sand (%)	Mz (φ)	Qz (%)	Fsp (%)	Cal (%)	Phl (%)	^{226}Ra (Bq/kg)	^{232}Th (Bq/kg)	^{40}K (Bq/kg)
1	E5 CAN01UP	22.0	5.58	28	25	12	33	29	48	920
	E1 CAN03UP	53.6	4.68	30	17	22	29	16	15	340
2	E12 CAN01UP	13.5	6.44	28	24	15	30	29	44	840
	E3 CAN03UP	14.3	6.46	25	23	22	29	24	37	750

4. Discussion

Multidisciplinary data sets from sedimentological analyses performed on the sediments from cores selected from the western gulf of Corinth provided information for the origin of the sedimentary deposits and the relative sedimentary processes.

The geological regime and the developed river network of the area suggest that the canyon receives sediments mainly from two river deltas; the Mornos river delta from the north and the Erineos Gilbert-type fan delta from the south. These two rivers drain the terrestrial formations ie. limestones and cherts of the alpine bedrock, Oligocene turbidites, Neogene conglomerates, sandstones, mudrocks and shales as well as Quaternary deposits (mostly deltaic and alluvial sediments). The mineral analysis of the cores showed the dominance of quartz, feldspars and phyllosilicate minerals against calcite thus implying these two rivers as source areas for the canyon sediments through the intensive erosion of the Neogene and Quaternary formations.

The study of the core sediments from the canyon of the western Gulf of Corinth provided undoubted evidences that for the last 900 years the sedimentary cover of the area is disturbed by a series of tubidite layers. The comparison of the turbititc events with the earthquake records of the area showed that the trigger mechanism could be the intense seismic activity of the area. This is further supported by the intense seismic activity recorded over the last 1000 years, characterized by strong seismic events (Mw > 5.8) which they may have triggered strong turbidite currents (Fig. 6). The impact of these events is considered to be so strong that they are related with breaks of the submarine cables (Heezen *et al*., 1966; Ferentinos *et al*., 1988).

Based on the interpretation of the pattern of turbidites in the canyon, Beckers (2015) has proposed two periods of seismic quiescence; 1740-1890 AD in the western part of the canyon and 1500-1700 AD in the eastern one. This coincident rather well with the findings of the present work. Two periods of seismic quiescence have been recorded between 1742-1869 AD and 1507-1674 AD in CAN01UP (western part) and CAN03UP cores (eastern part), respectively. This is probably due to the different sedimentation rates in the canyon, as well as the difference of the areas affected by the seismic epicenters and the acceleration of the seismic waves (Fig. 6). Both these factors can affect the extent of the turbidite horizons.

Although the comparison of these layers showed that the trigger mechanism could be the seismic activity of the area, the majority of the turbitic layers present an aseismic origin. The proximity of the coring sites to two major river fan deltas - these of Mornos and Erineos rivers- raises the enhanced river-discharging fluxes as additional origin for the turbitic events. A typical example is

the decade of 1920-1930 AD which is marked by four aseismic turbidite events in the CAN01UP sediment core. This series of turbitides may have been originated by enhanced weather conditions that led to increased sediment flux and accumulation of the river network of the canyon.

However the two coring locations present similar sedimentation motif as this is depicted by similarities in the mineral and radioactivity signature of both the hemipelagic and the turbiditic deposits. Dissimilarities occurred in the sedimentation rates and in the quantity of the turbiditic deposits. The western location (core CAN01UP) presented higher sedimentation rate together with higher number and longer total turbiditic deposits in relation to the eastern location (core CAN03UP). The above suggests that the competition among the sediment accumulation of the Mornos and Erineos rivers together with the bottom currents intensity and the seismic activity leads to the final sedimentary processes which most probably differs from west to east.

Figure 6 - Map showing the earthquake epicentres and the location of the two cores. Submarine cable breaks that were linked with earthquake shocks (according to Heezen *et al.*, 1966) are also highlighted.

5. Acknowledgments

This work resulted within our collaboration with Emer. Prof. Christian Beck (Savoie-Mont-Blanc University). Special thanks go to the crews of trawler *Eleni* and *R.V. Socrates* for their great and responsible work during the field work.

6. References

Avallone, A., Briole, P., Agatza-Balodimou, A.M., Billiris, H., Charade, O., Mitsakaki, C., Nercessian, A., Papazissi, K., Paradissis, D. and Veis, G., 2004. Analysis of eleven years of deformation measured by GPS in the Corinth Rift Laboratory area, *Comptes Rendus Geoscience*, 336, 301-311.

Beckers, A., 2015. Late Quaternary sedimentation in the western tip of the Gulf of Corinth, Universite de Liege, PhD thesis.

Beckers, A., Hubert-Ferrari, A., Beck, C., Bodeux, S., Tripsanas, E., Sakellariou, D. and De Batist, M., 2015. Active faulting at the western tip of the Gulf of Corinth, Greece, from high-resolution seismic data, *Marine Geology*, 360, 55-69.

Briole, P., Rigo, A., Lyon-Caen, H., Ruegg, J.C., Papazissi, K., Mitsakaki C., Balodimou A., Veis G., Hatzfeld D. and Deschamps A., 2000. Active deformation of the Corinth rift, Greece: Results from repeated Global Positioning System surveys between 1990 and 1995, *Journal of Geophysical Research*, 105, 25605-25625.

Doutsos, T., Kontopoulos, N. and Poulimenos, G., 1988. The Corinth-Patras rift as the initial stage of continental fragmentation behind an active island arc (Greece), *Basin Research*, 1, 177-190.

Ferentinos, G., Papatheodorou, G. and Collins, M.B., 1988. Sediment transport processes on an active submarine fault escarpment: Gulf of Corinth, Greece, *Marine Geology*, 83, 43-61.

Heezen, B.C., Ewing, M. and Johnson, L., 1966. The Gulf of Corinth floor, *Deep-Sea Research*, 13, 381-411.

Jackson, J. and McKenzie, D., 1988. The relationship between plate motions and seismic moment tensors and the rates of active deformation in the Mediterranean and Middle East, *Journal of Geophysics*, 93, 45-73.

Lykousis, V., Sakellariou, D., Nonikou, P., Alexri, S., Rousakis, G., Georgiou, P., Kaberi, E. and Balas, D., 2007b. Sediment failure processes in active grabens: The Western Corinth Gulf (GREECE). *In:* Lykousis, V., Sakellariou, D. and Locat, J., *eds.*, Submarine mass movements and their consequences III. Advances in natural and technological hazards research, Springer, Dordrecth, 424 pp.

Makris, J., 1976. A dynamic model of the Hellenic arc deduced from geophysical data, *Tectonophysics*, 36, 339-346.

McKenzie, D.P., 1972. Active tectonics of the Mediterranean region, *Geophysical Journal of the Royal Astronomical Society*, 30, 109-182.

McKenzie, D.P, 1978. Active tectonics of the Alpine-Himalayan belt: the Aegean Sea and surrounding regions, *Geophysical Journal of the Royal Astronomical Society*, 55, 217-254.

Moretti, I., Sakellariou, D., Lykousis, V. and Micarelli, L., 2003. The Gulf of Corinth: an active half graben?, *Journal of Geodynamics*, 36, 323-340.

Papadopoulos, G.A., 2003. Tsunami Hazard in the Eastern Mediterranean: Strong Earthquakes and Tsunamis in the Corinth Gulf, Central Greece, *Natural Hazards*, 29, 437-464.

Papatheodorou, G. and Ferentinos, G., 1997. Submarine and coastal sediment failure triggered by the 1995 Ms=6.1R Aegion earthquake, Gulf of Corinth, Greece, *Marine Geology*, 137, 287-304.

Papazachos, B.C. and Comninakis, P.E., 1971. Geophysical and tectonic features of the Aegean arc, *J. geophys. Res*., 76, 8517-8533.

Perissoratis C., Piper D.J.W. and Lykousis V., 2000. Alternating marine and lacustrine sedimentation during late Quaternary in the Gulf of Corinth rift basin, central Greece, *Marine Geology*, 167, 391-411.

Piper, D.J.W., Kontopoulos, N., Anagnostou, C., Chronis, G. and Panagos, A.G., 1990. Modern Fan deltas in the Western Gulf of Corinth, *Geo-Marine Letters*, 10, 5-12.

Poulos S., Collins M., Pattiaratchi C., Cramp A., Gull W., Tsimplis M. and Papatheodorou G., 1996. Oceanography and sedimentation in the semi-enclosed, deep water gulf of Corinth (Greece), *Marine Geology*, 134, 213-235.

Stefatos, A., Papatheodorou, G., Ferentinos, G., Leeder, M. and Collier, R., 2002. Seismic reflection imaging of active offshore faults in the Gulf of Corinth: their seismotectonics significance, *Basin Research*, 14, 487-502.

Zelilidis, A., 2003. The geometry of fan-deltas and related turbidites in narrow linear basins, *Geological Journal*, 38, 31-46.

http://www.emidius.eu/SHEEC/. The SHARE European Earthquake Catalogue.